

Short note

The angular distribution of the $^{12}\text{C}(\gamma,\text{pn})$ reaction for $E_\gamma = 120 - 150$ MeV

T.T.-H. Yau^{1,a}, I.J.D. MacGregor¹, J. Ahrens⁴, J.R.M. Annand¹, R. Beck⁴, D. Branford², P. Grabmayr³, S.J. Hall¹, P.D. Harty^{1,b}, T. Hehl³, D.G. Ireland¹, J.D. Kellie¹, T. Lamparter³, K. Livingston¹, M. Liang^{2,c}, J.A. MacKenzie², S. McAllister¹, J.C. McGeorge¹, R.O. Owens¹, M. Sauer³, R. Schneider³, D.P. Watts¹

¹ Department of Physics and Astronomy, University of Glasgow, Glasgow G12 8QQ, UK

² Department of Physics and Astronomy, University of Edinburgh, Edinburgh EH9 3JZ, UK

³ Physikalisches Institut, Universität Tübingen, D-72076 Tübingen, Germany

⁴ Institut für Kernphysik, Universität Mainz, D-55099 Mainz, Germany

Received: 3 September 1997 / Revised version: 17 December 1997

Communicated by Th. Walcher

Abstract. The angular distribution of nucleons emitted in the $^{12}\text{C}(\gamma,\text{pn})$ reaction has been measured using tagged photons at the Mainz microtron MAMI. The variation of the reaction strength with the polar angles of the two emitted nucleons is reported for $E_\gamma = 120 - 150$ MeV. The proton angular distribution peaks at more backward angles than the $^2\text{H}(\gamma,\text{p})$ differential cross section indicating a departure from the simple quasi-deuteron model of 2N photo-emission. The distribution shape is in reasonable agreement with microscopic theoretical models which include both π - and ρ -exchange.

PACS. 21.30.Fe Forces in hadronic systems and effective interactions – 25.20.Lj Photoproduction reactions – 27.20.+n $6 \leq A \leq 19$

The atomic nucleus is a many body quantum mechanical system in which the constituent nucleons are bound at long and medium range by the exchange of virtual mesons. These interactions can be probed by studying two nucleon knockout reactions induced by real or virtual photons. At low missing energies the strong (γ,pn) channel has been shown to be well described by photon absorption on a proton-neutron pair with the remaining nucleons acting as spectators to the reaction [1–3]. At these missing energies little distortion from final state interactions (FSI) is observed and the outgoing nucleons have a strong angular correlation which is determined by 2N photoemission kinematics, smeared out by the initial Fermi motion of the participating nucleons. Strong similarities have been observed between the (γ,pn) reaction in light nuclei and the $^2\text{H}(\gamma,\text{pn})$ reaction. The photon energy dependence of the (γ,pn) reaction in light nuclei, at low or moderate excitation of the residual nucleus, [4–6] has the same shape as the deuterium photodisintegration reaction and the outgo-

ing nucleons have similar angular correlations [1–3]. These observations have suggested that the major features of 2N photoemission reactions are well described by the simple quasideuteron model [7].

Microscopic calculations [8–11] of the coupling of the virtual mesons to external electromagnetic fields provide more detailed insight into the meson exchange mechanisms in nuclei. One-pion-exchange (OPE) processes are dominant but recent calculations have also studied the contributions from the exchange of heavier mesons. Detailed (γ,NN) measurements, which are now being made in the few hundred MeV photon energy region, are being compared with these increasingly complete calculations to see if any features emerge which cannot be explained within the standard nucleon-meson framework and which might indicate shorter range effects.

Recent calculations of (γ,pn) cross sections in light nuclei by the Gent group [8–11] at photon energies up to ~ 150 MeV have suggested that the angular distribution of the two outgoing nucleons can be used to assess the different contributing mesonic exchange mechanisms. The kinematics of 2N photon absorption gives two nucleons emitted back-to-back in the centre-of-mass frame of the photon and the interacting pair. In the laboratory frame this results in a pronounced ridge in a 2-D plot of the

^a Present address: Chase Research, Basingstoke, UK

^b Present address: Physics Dept., University of Auckland, New Zealand

^c Present address: Thomas Jefferson Lab, Newport News, USA

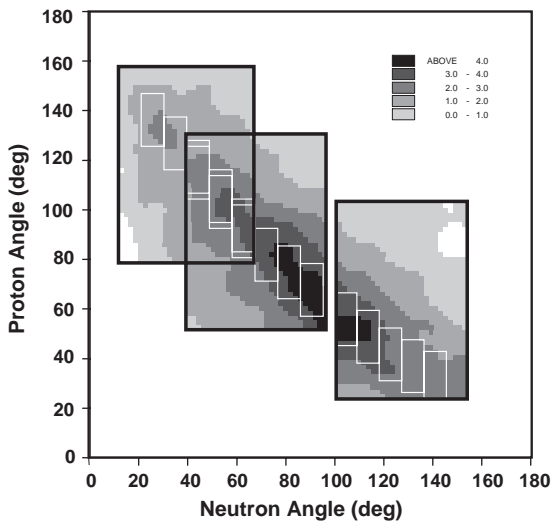


Fig. 1. $^{12}\text{C}(\gamma,\text{pn})$ differential cross section as a function of θ_p and θ_n for $E_\gamma = 120 - 150$ MeV and $E_m = 20 - 70$ MeV, showing the angular coverage obtained in three separate detector settings and a schematic representation (small white rectangles) of the proton and neutron polar angular bins used for further analysis. The relative magnitude of the observed cross sections are shown using a linear scale

cross section as a function of the proton (θ_p) and neutron (θ_n) polar angles, as reflected by the experimental data plotted in Fig. 1, and the variation in the strength of the cross section along this ridge is sensitive to the contributing meson exchange terms. The calculated distributions depend on the current operators and are significantly different for the ‘ π -seagull’ and ‘ π -in-flight’ terms. The shape of the ‘ ρ -seagull’ angular distribution [11] is similar to the π -seagull distribution indicating that the mediating meson is less important than the type of process (seagull or meson-in-flight) involved.

The Gent calculations show that the most important pionic exchange terms are the π -seagull and the π -in-flight terms [8, 10]. Either term on its own has an angular distribution with a maximum at nucleon angles near 90° , but their interference produces a reduction in the magnitude of the cross section and a shallow minimum at these central angles. A recent investigation including heavier mesons [9, 11] shows that the ρ -seagull term also has a significant effect. Interference between the π currents and the ρ -seagull term reduces the cross sections, particularly at the extreme forward and backward angles, leaving a broad maximum at central nucleon angles.

The general expectation from the Gent calculations is that the angular distribution of the (γ,pn) reaction will be a valuable probe of the contributing meson exchange mechanisms. This letter reports results from the first measurement of the (γ,pn) angular distribution. Data for the $^{12}\text{C}(\gamma,\text{pn})$ reaction for the photon energy range $E_\gamma = 120 - 150$ MeV and for missing energies $E_m = 20 - 70$ MeV are compared with the differential cross section for the

$^2\text{H}(\gamma,\text{p})$ reaction and with (γ,pn) calculations published by the Gent group [11].

The experiment was performed using the Glasgow photon tagging spectrometer [12] at the 855 MeV Mainz microtron [13]. The target consisted of a $0.7\text{g}/\text{cm}^2$ graphite sheet at 30° to the photon beam. A plastic scintillator hodoscope PiP [14] was used to detect protons. In three separate angular settings it covered polar angles $\theta_p = 23^\circ - 157^\circ$ with a resolution of $\sim 3.5^\circ$. Coincident neutrons were detected in 96 plastic scintillator time-of-flight (TOF) detectors [15] arranged in 4 layers, at an average distance of ~ 6 m from the target. At each setting of PiP these were positioned on the opposite side of the beam at the complementary angle for deuterium photodisintegration kinematics. The three TOF positions covered $\theta_n = 11^\circ - 153^\circ$ with a resolution of $\sim 2^\circ$. The detector calibration procedures and the method of analysis are described in detail in [16]. The detector system has a missing energy resolution of ~ 8 MeV. A cut of $E_m \leq 70$ MeV was used to select events arising predominantly from direct 2N photoemission [2, 3, 17]. This cut includes nucleon pairs emitted from both $(1p)^2$ and $1p1s$ shells.

Figure 1 is a contour plot of the measured differential cross section as a function of θ_p and θ_n which shows the coverage obtained in the three separate PiP-TOF detector settings. The data are distributed in a ‘ridge’, corresponding to quasideuteron kinematics, spread out by the Fermi motion of the initial pair. To measure the strength along the ridge angular bins were chosen to straddle the top of the ridge, as outlined in the figure. At each angular setting data from groups of 16 TOF detectors (4 bars wide \times 4 layers deep) were combined to form neutron angular bins. The width of each bin was $\Delta\theta_n \sim 7.5^\circ$. The solid angles $\Delta\Omega_n$ were calculated from $\Delta\theta_n$ and the full azimuthal acceptance of the TOF detectors. Proton angular bins of width $\Delta\theta_p = 20^\circ$ were centered about the corresponding mean proton angles θ_p . The size of these bins reflected the width of the ridge in Fig. 1 and the solid angles $\Delta\Omega_p$ included the full azimuthal range of PiP.

The results of the Gent calculations are in the form of double differential cross sections, $d^2\sigma/d\Omega_p d\Omega_n$, along the top of the ridge in Fig. 1. The measured double differential cross sections are averaged over finite bins which contain polar angle pairs and azimuthal angle pairs for which the cross section falls below these top-of-the-ridge values, due to spreading of the reaction strength arising from Fermi motion of the initial nucleons. To obtain the peak cross sections shown in Fig. 2 from the measured average values a simple correction factor has been calculated to account for the angular variation of the cross section within each bin. A Gaussian distribution, of width 40° HWHM, was used to model the Fermi cone. The large width reflects the low mean energies of the emitted nucleons when averaged over the accepted range of residual excitation energies. This gave a normalisation factor of ~ 1.15 for each bin when averaged over the detector angular acceptances. This factor was almost constant over the entire angular range of our data.

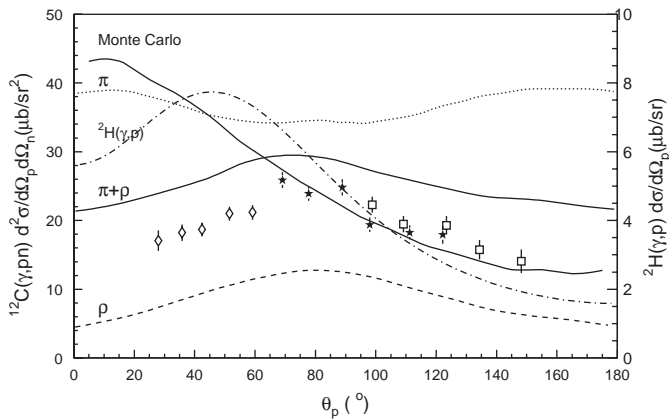


Fig. 2. $^{12}\text{C}(\gamma,\text{pn})$ differential cross section (LH scale) along the top of the ridge in Fig.1 as a function of θ_p for $E_\gamma=120-150$ MeV and $E_m=20-70$ MeV. The *diamonds*, *stars* and *squares* represent data taken in three separate detector positions. Also shown are Gent calculations [11] for $^{16}\text{O}(\gamma,\text{pn})$ at $E_\gamma=140$ MeV in coplanar kinematics which have been multiplied by 0.75, as described in the text, to account for the differences between ^{12}C and ^{16}O . The *dotted line* is the π exchange contribution, including both π -seagull and π -in-flight terms. The *dashed line* is the ρ -seagull contribution and the *thick solid line* is the coherent sum of the π and ρ currents. The *dot-dashed line* (RH scale) is the parameterisation by Jenkins *et al.* [19] of the $^2\text{H}(\gamma,\text{p})$ differential cross section at $E_\gamma=135$ MeV. The *thin solid line* is the result of a Monte Carlo model including the effects of Fermi motion and differences in emitted nucleon energies between $^2\text{H}(\gamma,\text{p})\text{n}$ and $^{12}\text{C}(\gamma,\text{pn})$

Figure 2 shows good agreement between the data from the three separate angular settings. The shape of the distribution shows a maximum at proton angles of $\sim 80^\circ$, which is close to the symmetric case of nearly equal proton and neutron angles, corresponding to approximately 90° in the centre-of-mass system of the photon and the initial pair.

The dot-dashed line (RH scale) in Fig. 2 shows the parameterisation by Jenkins *et al.* [19] of the experimental $^2\text{H}(\gamma,\text{p})$ angular distribution at $E_\gamma = 135$ MeV. In order to investigate how the effects of Fermi motion, the difference in nucleon binding energies between $^2\text{H}(\gamma,\text{pn})$ and $^{12}\text{C}(\gamma,\text{pn})$ and the excitation of the residual nucleus would affect this curve a Monte Carlo simulation was carried out using the 2N photoabsorption model described by McGeorge *et al.* [2]. The results, shown by the thin solid line in Fig. 2, allowed the same range of residual excitation as the analysed data. The curve is slightly flatter due to Fermi motion, but the largest effect is a shift to forward proton lab angles which is attributed to the reduction in energy of the outgoing nucleons. It is evident that the $^2\text{H}(\gamma,\text{p})\text{n}$ distribution has a different shape to that for the $^{12}\text{C}(\gamma,\text{pn})$ data whether or not the pair momentum and differences in the outgoing nucleon energies are accounted for. Calculations of the deuterium photodisintegration cross section at 140 MeV [21] which include both relativistic effects and heavy meson exchange show that the dominant contribu-

tion comes from OPE with destructive interference from ρ -exchange reducing the cross section by $\sim 20\%$ at extreme forward and backward angles.

The difference in the shapes between ^2H and ^{12}C shows for the first time that the (γ,pn) reaction in complex nuclei is not just a simple quasideuteron scaling of the same reaction in deuterium. It indicates significant differences in the 2N photoemission mechanism between ^2H and ^{12}C which may be due to the different relative importance of π -seagull, π -in-flight, ρ exchange or short range effects in ^{12}C compared to the more diffuse deuterium nucleus.

Up till now the published theoretical angular distribution calculations in light nuclei have been restricted to ^{16}O and these have been used for comparison with the present data. The calculations used an unfactorized model of the (γ,pn) reaction using plane waves for the outgoing particles. It is expected [18] that the $^{16}\text{O}(\gamma,\text{pn})$ calculations, suitably normalised, will be a good guide to the effects of different reaction mechanisms in ^{12}C since the nuclear structure ingredients for both nuclei are rather similar. For comparison with the present $^{12}\text{C}(\gamma,\text{pn})$ data the published theoretical calculations for $^{16}\text{O}(\gamma,\text{pn})$ have been renormalised by a factor of 0.75 based on the probability NZ/A of finding neutron-proton pairs from either 1p or 1s shells in the two nuclei. This recipe, when applied to $(1\text{p})^2$ emission, is consistent with previous measurements of ^{12}C and $^{16}\text{O}(\gamma,\text{pn})$ cross sections at missing energies below 40 MeV and 43 MeV respectively [2,20]. The result is shown in Fig. 2. The comparison between the calculations and the data shows that the $\pi + \rho$ calculation gives a much better representation of the shape of the measured angular distribution than the π terms alone. The magnitude of the data is less than the $\pi + \rho$ calculation although the scaling of the ^{16}O calculations has brought the theoretical prediction much closer to the data. It should be noted that the calculations shown in Fig. 2 do not include contributions from Δ currents which may contribute $\sim 30\%$ to the total cross section at the present energies [11].

These first results indicate the need for specific calculations for ^{12}C over a wide kinematic range taking into account the finite acceptance of the nucleon detectors. Such calculations, compared to data over the full range of energies ($E_\gamma=120-400$ MeV) measured in the present experiment, will provide a much clearer picture of all the contributing mechanisms, although the clearest evidence of effects due to exchange of heavy mesons may be at the energies reported here ($E_\gamma < 150$ MeV) which are not dominated by Δ -currents.

This work was supported by the UK EPSRC, the British Council, the DFG (Mu 705/3), BMFT (06 Tü 656), DAAD (313-ARC-VI-92/118), the EC (SCI.0910.C(JR)) and NATO (CRG 920171). The authors would like to thank the Institut für Kernphysik der Universität Mainz for the use of its facilities and for the generous assistance provided during the course of this experiment. T.T.-H.Y., J.A.M., S.M. and D.P.W. would like to thank EPSRC for research studentships during the period of this work.

References

1. S. N. Dancer et al., Phys. Rev. Lett. **61**, 1170 (1988)
2. J. C. McGeorge et al., Phys. Rev. C **51**, 1967 (1995)
3. P. D. Harty et al., Phys. Lett. B **380**, 247 (1996)
4. M. Kanazawa et al., Phys. Rev. C **35**, 1828 (1987)
5. R. Wichmann et al., Z. Phys. A **335**, 169 (1996)
6. P. Grabmayr et al., Phys. Lett. B **370**, 17 (1996)
7. J.S. Levinger, Phys. Rev. **84**, 43 (1951)
8. J. Ryckebusch et al., Phys. Lett. B **291**, 213 (1992)
9. L. Machenil et al., Phys. Lett. B **316**, 17 (1993)
10. J. Ryckebusch et al., Nucl. Phys. A **568**, 828 (1994)
11. M. Vanderhaegen et al., Nucl. Phys. A **580**, 551 (1994)
12. S. J. Hall et al., Nucl. Inst. Meth. A **368**, 698 (1996);
I. Anthony et al., Nucl. Inst. Meth. A **301**, 230 (1991)
13. H. Herminghaus, *Proc. of the Linear Accelerator Conference*, Albuquerque, USA, (1990).
T. Walcher, Prog. Part. Nucl. Phys. **24**, 189 (1990)
14. I. J. D. MacGregor et al., Nucl. Inst. and Meth. A **382**, 479 (1996)
15. P. Grabmayr et al., *Proc. of the Workshop on Future Detectors for Photonuclear Experiments*, Edinburgh, Scotland, p225 (1991)
16. T. T.-H. Yau, Ph.D. thesis, University of Glasgow, (1996)
17. T. Lamparter et al., Z. Phys. A **355**, 1 (1996)
18. J. Ryckebusch, private communication
19. D. A. Jenkins, P. T. Debevec and P. D. Harty, Phys. Rev. C **50**, 74 (1994)
20. I. J. D. MacGregor et al., Nucl. Phys. A **533**, 269 (1991)
21. F. Ritz, H. Arenhövel and T. Wilbois, to be published